Weather, Climate Change, and Land Use:

A High-Resolution Analysis in China

Jianghao Wang
Chinese Academy of Sciences, and MIT
wangjh@mit.edu

Junjie Zhang
Duke Kunshan University, and Duke University
junjie.zhang@duke.edu

Peng Zhang
The Hong Kong Polytechnic University
peng.af.zhang@polyu.edu.hk

Abstract

Climate change is a major threat to food security. The determination of policy actions requires accurate estimates of climatic impacts on both crop yields (intensive margin) and cropland area (extensive margin). However, the analysis on the latter has been limited, especially in developing countries. This paper assesses the impact of temperature on land use in China by matching high-resolution satellite data of land use with daily weather data from 1980 to 2010. We find extremely hot weather (daily average temperature above 30 ℃) has a long-lasting effect on reducing cropland in China. In addition, we find that non-irrigated land is more susceptible to rising temperatures in the short term; however, irrigated land is subject to a similar impact in the long term. This result suggests that the adaptive effect of irrigation could be limited under persistent rising in temperature.

JEL Codes: O13, O44, Q15, and Q54.

Keywords: Weather, Climate Change, Land Use, and China.

Acknowledgements: We thank Christopher Costello, Olivier Deschenes, Kyle Meng, as well as seminar participants at UC Santa Barbara, The Hong Kong Polytechnic University, Shandong University, Southwestern University of Finance and Economics, South China Normal University, and Renmin University of China for helpful comments. This work was supported by the Strategic Priority Research Program of Chinese Academy of Sciences (No. XDA19040503) and the National Natural Science Foundation of China (No. 41971409, 71773043, 71773062). Any remaining errors are our own.

1 Introduction

Sustaining food security has become a major development goal worldwide as the global population is rapidly increasing, more crops are being converted into biofuels, and newly developing economies are switching to more resource-intensive food such as meat. Climate change has emerged as a new threat to global food security (Schmidhuber et al., 2007; Godfray et al., 2010). Changes in climatic conditions, such as higher temperatures and shifted precipitation patterns, negatively affect the production of staple food crops. Besides crop yields (intensive margin), long-term and gradual climate change will also fundamentally affect cropland area (extensive margin) as cropland becomes less arable and less profitable (Larson et al., 2013).

To date, most economics studies have focused on crop yields, or crop production per acre (e.g., Deschenes and Greenstone, 2007; Schlenker and Roberts, 2009; Burke and Emerick, 2016; Zhang et al., 2017). Studies on cropland area are limited, with only a few exceptions focused on developed countries (Haim et al., 2011; Fezzi et al., 2015). Developing countries, on the other hand, could face larger threat from climate change as they have insufficient resources to adapt and greatly rely on ecological systems (Tol, 2018).

This paper estimates the impact of temperature on land use in China. China is an important context to study for several reasons. First, China has 20% of the world's population, but has only 7% of its cropland (World Bank, 2019). Second, the rapid urbanization and the rising demand for calories and protein further pose significant

challenges to China's food security. In fact, China is struggling to maintain at least 1.2 million km^2 cropland; the so-called "red line" is arguably the minimum amount of cropland needed to feed the Chinese people (Kong, 2014). Lastly, China is the largest grain producer and importer. Therefore, adverse climatic effects on China' land use could lead to a ripple effect that ultimately endangers the global food security.

We construct a unique dataset that combines high-resolution satellite data on land use together with daily weather data. In particular, the satellite data on land use report the areas of six land types—cropland (irrigated and non-irrigated), forest land, grassland, waterbody, developed land, and barren land—at a resolution of 10×10-km grid in the years of 1980, 1995, 2000, 2005, and 2010. Utilizing the satellite data give us at least three advantages. First, the data provide relatively reliable estimates since the reported statistics in land areas are subject to data manipulation by local governments. Second, the 30-year period enables us to assess the long-term impacts of weather on land use. Finally, the cross-sectional variation is rich as the data contain 96,421 grids with 482,105 observations in total.

To capture the non-linear effects of temperature, we divide daily average temperature into 5 ℃ bins starting from below minus 10 ℃ to above 30 ℃, and then count the number of days within each bin in each year. This semi-parametric approach is widely used in the literature, which is flexible in the functional form and keeps daily variations (Deschenes and Greenstone, 2011).

We use three methods to measure the long-term effect of temperature on land use. The first method is a distributed-lag model, which we include both contemporaneous and lagged temperature bins, up to 10 years. We then sum the coefficients for all lags and interpret the summation as the cumulative effects of a sequence of temperature bins across years. This method, widely adopted by the climate-economy literature, is very flexible in estimating long-term effects (Dell et al., 2012).

The second method is a period-averaged model, in which we average temperature bins from lagged years to the contemporaneous year. This method is similar to the distributed-lag model. Lastly, we use the long differences model (Burke and Emerick, 2016), which regresses the differenced temperature bins on the differenced land area between 1980s and 2010s. This method is similar to the period-averaged model but uses longer time variation.

We find extremely hot weather (daily average temperature above 30 ℃) has a long-lasting effect on reducing cropland in China. In particular, if climate change increases temperature of one day from 15–20 ℃ to above 30 ℃ permanently, it reduces cropland area by a total of 1.01% in 10 years. The results are robust across all three models. In addition, we find that non-irrigated land is more susceptible to rising temperatures in the short term (less than 5 years); however, irrigated land is subject to a similar impact in the long term (more than 5 years). This result suggests that the adaptive effect of irrigation could be limited under persistent temperature increase. We find insignificant temperature effects for forestland, grassland, waterbody, and barren

land. However, the effect of extremely hot weather on developed land (used for urban and rural residence, infrastructure, and industry) is significantly positive. It suggests that some lost cropland has been converted to developed land.

Finally, combining climate projections from 39 downscaled climate models, we predict that climate change is likely to reduce China's cropland area by 2.09%–25.51% under IPCC's slowest and fastest warming scenarios by the end of this century. This suggests that climate change could threaten China's cropland. China, the world's largest CO_2 emitter, could take more aggressive climate actions in its own interest.

2 Data

2.1 Land Data

The land data are from China's Land-Use/Cover Datasets (CLUDs), which are provided by the Data Center for Resources and Environmental Sciences at the Chinese Academy of Sciences. CLUDs were updated from 1980 to 2010, with standard procedures based on satellite images as well as visual interpretation and digitalization at a spatial resolution of 10×10-km grid. The data report the percentages of six main land categories, including cropland, forest land, grassland, waterbody, developed land, and barren land in the years of 1980, 1995, 2000, 2005, and 2010. The primary focus of this paper is cropland, which is further classified as irrigated or non-irrigated cropland.

Figure 1 shows the geographic distribution of China's cropland (panel A), irrigated (panel B) and non-irrigated cropland (panel C), and developed land (panel D) in 2010. The color shows the percentage of each land type in a 10×10-km grid. Although China is the third largest country in the world in terms of land area, almost half of China's land is not suitable for agriculture, particularly in Xinjiang, Qinghai, and Xizang. Non-irrigated land is mostly located in the north and northeast, including Heilongjiang, Neimenggu, Shandong, Hebei, and Henan. In contrast, irrigated land is mostly located in the south, particularly in Jiangsu, Anhui, Sichuan, Hunan, and Hubei. Overall, the majority of cropland in China is non-irrigated. These main grain production areas are also under rapid industrialization and urbanization.

[Insert Figure 1 here]

Panel A of Table 1 reports the summary statistics for cropland and developed land area in square kilometers within each 10×10-km grid during 1980–2010. On average, cropland accounts for 18% of total land, and 70% of cropland is non-irrigated. Developed land accounts for around 2% of total land in China.

[Insert Table 1 here]

2.2 Weather and climate prediction data

The weather data are drawn from China Meteorological Data Service Center. It has been publishing daily weather data including maximum and minimum temperatures, precipitation, relative humidity, wind speed, and sunshine duration for more than 800 weather stations across China since 1951. We use the kriging spatial

prediction method (Cressie and Wikle, 2015) to covert weather data on each day from each station to a 10×10-km grid to match with the land use data.

To measure the non-linear effects of temperature, we follow the bins approach (Deschenes and Greenstone, 2011), and divide daily average temperature (average between daily maximum and minimum temperatures) into 5 ℃ bins starting from minus 10 ℃ to above 30 ℃. The bin 15–20 ℃ severs as the reference group. We then count the number of days within each bin. We use the annual mean plus a quadratic term for relative humidity, wind speed, and sunshine duration; we also use the annual total with a quadratic term for precipitation. Note that we use weather variables for all days in a year. In comparison, the literature that measures weather effects on crop yields only considers the weather in the growing seasons. This is mainly because we do not know which crops are planted in each grid.

Panel B of Table 1 reports the average number of days within each 5 ℃ temperature bin in China during 1970–2010. Most days lie within 10–25 ℃. On average, China has 1.89 extreme hot days with daily average temperature above 30 ℃ per year. Panel C further reports the average for precipitation, relative humidity, sunshine duration, and wind speed.

The climate prediction data are drawn from the Coupled Model Intercomparison Project 5 (Taylor et al., 2012). We obtain the mean prediction on daily average temperature from 39 climate models under Representative Concentration Pathways (RCPs) 2.6 (slowest scenario), 4.5, 6.0, and 8.5 (fastest scenario) for each 2.5×2.5-

degree grid for each month over the period 1970–2010 and 2070–2099. We then calculate the temperature difference in each month-grid between two periods and convert from a 2.5×2.5-degree grid to a 10×10-km grid using the area-to-point downscaling (Kyriakidis, 2004) method to match with historical weather data. We add the difference to the observed daily time series from 1970–2010. This shifts the mean of daily temperature but also keeps its variance so that we can predict the number of days within each temperature bin (Auffhammer et al., 2017).

Figure 2 plots the historical (1970–2010) and predicted (2070–2099) histograms under four RCPs, ranging from the slowest (RCP 2.6) to the fastest (RCP 8.5) warming scenario. It shows that climate change shifts the distribution of temperature to a higher range. As a result, more extremely hot weather, with daily average temperature above 30 ℃, are likely to occur. For example, annual extreme hot days will increase from 2 to 22 days on average in China under the fastest warming scenario by the period of 2070–2099.

[Insert Figure 2 here]

3 Econometric Model

We have developed three econometric models to estimate the effect of temperature on land area. The first model, which is also the baseline model, is a distributed-lag model. Let i index 10×10-km grid and t index year (1980, 1995, 2000, 2005, and 2010). The natural log of cropland area in year t is a function of

$$ln\, y_{it} = \alpha + \sum_{j=0}^{J}(\sum_b \beta_j^b T_{it-j}^b) + \sum_{j=0}^{J}(\gamma_j' \boldsymbol{W}_{it-j}) + \delta_i + \lambda_{pt} + \varepsilon_{it}, \quad (1)$$

where T^b is the number of days in temperature bin b. Daily average temperature (the average between daily maximum and minimum temperatures) is specified as 5 ℃ bins starting from below minus 10 ℃ to above 30 ℃, with 15–20 ℃ as the reference. This specification allows for flexible temperature-land relationships (Deschenes and Greenstone, 2011). The vector of other weather variables, $\boldsymbol{W}$, includes total precipitation, average relative humidity, average wind speed, and average sunshine duration, in both linear and quadratic terms. Both T^b and $\boldsymbol{W}$ are included with J lags, where J ranges from 0 to 10 years. We do not further extend 10-year lags as we believe 10 years is a reasonable long-term exposure window. This is also consistent with Dell et al. (2012), who used a 10-year distributed lagged model to study the long-term climate-economy relationship.

We use δ_i, grid fixed effect, to control for time-invariant grid-specific characteristics such as geographic location and soil quality. We use year-by-province fixed effect, λ_{pt}, to control for common shocks within each province in a year such as technological progress, policy change, and crop prices shocks. The unobservable error term ε_{it} is clustered at the 10×10-km grid level to allow for arbitrary spatial and serial correlations within each grid. Our results are robust if standard errors are clustered at a more aggregated level, including county (the size of a typical county is 50×50 km) and prefecture (a typical prefecture includes 10 to 20 counties).

The distributed lag model can generate unbiased estimates of climatic impacts (Dell et al., 2012). The regression of this model will be run separately for J times, with

J from 0 to 10 years of lag. The parameter of central interest is $\sum_j^J \beta_j^b$, which measures the J-year cumulative effect of temperature bin b on cropland area. Suppose climate change permanently shifts one day within 15–20 ℃ to temperature bin b. Other things being equal, it will change cropland area by $\sum_j^J \beta_j^b$ in percentage points, accounting for both contemporaneous and lagged effects up to J years.

The second model is a period-averaged model that uses the averages of each weather variables in contemporaneous and lagged years. Specifically, the natural log of area for grid i in year t is a function of

$$\ln y_{it} = \alpha + \sum_b \beta^b \overline{T_i^b} + \gamma' \overline{\boldsymbol{W}_i} + \delta_i + \lambda_{pt} + \varepsilon_{it}, \quad (2)$$

where

$$\overline{T_i^b} = \frac{1}{J+1} \sum_{j=0}^{J} T_{it-j}^b, \text{ and}$$

$$\overline{\boldsymbol{W}_i} = \frac{1}{J+1} \sum_{j=0}^{J} \boldsymbol{W}_{it-j}.$$

In the model, all weather variables are calculated using the average of J lagged years, with J from 0 to 10 years. The other notations are the same as those in Equation (1). The parameter of central interest is β^b, which measures the J-year cumulative effect of temperature bin b on cropland area. The regression of Equation (2) will be run separately for J times, with 0 to 10 years of lag.

The third model is a long differences model following Burke and Emerick (2016):

$$\Delta \ln y_i = \alpha + \sum_b \beta^b \Delta \overline{T_i^b} + \gamma' \Delta \overline{\boldsymbol{W}_i} + \lambda_p + \varepsilon_i \quad (3).$$

In this form, $\Delta \ln y_i$ measures the difference in log of land area between 1980 and 2010, i.e., $\Delta \ln y_i = \ln y_{i,2010} - \ln y_{i,1980}$. Ideally, we want to use the average of log land area spanning several years across two long periods, such as the average over the period 1978–1982 and 2008–2012, but the land data are only available in 1980 and 2010. Correspondingly, $\Delta\overline{T_i^b}$ and $\Delta\overline{\boldsymbol{W}_i}$ measure the difference in averaged temperature and other weather variables between 1980 and 2010, such that

$$\Delta\overline{T_i^b} = \frac{1}{J+1}\sum_{j=0}^{J} T_{i,2010-j}^b - \frac{1}{J+1}\sum_{j=0}^{J} T_{i,1980-j}^b, \text{ and}$$

$$\Delta\overline{\boldsymbol{W}_i} = \frac{1}{J+1}\sum_{j=0}^{J} \boldsymbol{W}_{i,2010-j} - \frac{1}{J+1}\sum_{j=0}^{J} \boldsymbol{W}_{i,1980-j}.$$

The province fixed effect in Equation (3) is denoted by λ_p. The other notations are the same as those in Equation (1). The regression of Equation (3) will be run separately for J times, with 0 to 10 years of lag. The parameter of central interest is β^b, which measures the J-year cumulative effect of temperature bin b on cropland area. The difference between Equations (2) and (3) is that the latter uses longer variation.

4 Results

4.1 Historical impact of temperature on cropland area

We start with the distributed-lag model (Equation (1)) and plot the estimated relationships between temperature and cropland area, with 95% confidence intervals, in Figure 3. The estimate is interpreted as the J-year cumulative effect of temperature on cropland, with J denoting the lags up to 10 years. Take the result of the 10-year model (lag 10) as an example. If climate change increases temperature of one day from 15–20 ℃ to above 30 ℃ permanently, it reduces cropland area by a total of 1.01% in

10 years. Since heat and extremely hot weather will rise significantly under climate change (Figure 2), this estimate implies significant risk of cropland loss.

[Insert Figure 3 here]

The temperature-cropland relationship is non-linear. In general, temperature below 30 ℃ has a limited effect; temperature above 30 ℃ has a statistically significant and economically large effect on cropland loss. In addition, the negative effect of extremely hot days increases when more lags are included, suggesting temperature has a long-lasting cumulative effect.

Table 2 reports the estimates for other weather variables other than temperature, including precipitation, relative humidity, sunshine duration, and wind speed. We also include the quadratics for non-linearity. In general, the effects are statistically insignificant, except only for a few specifications.

We then test the robustness of our results. First, we test for different model specifications. Our baseline model uses a distributed-lag model. Alternatively, Figure 4 (Equation (2)) plots the estimated coefficients with the 95% confidence intervals using the period-averaged model. The estimates mimic the findings in Figure 3. In Figure 5, we estimate the model using the long differences method (Equation (3)). We also find very similar impacts.

[Insert Figure 4 here]

[Insert Figure 5 here]

Second, we test for different measurements of daily temperature. In the baseline model, we construct bins using daily average temperature. Alternatively, we construct bins using daily maximum and minimum temperatures respectively. To better use the variation in tails, we define extremely hot weather as the daily maximum temperature above 35 ℃ and daily minimum temperature above 25 ℃. The estimates are plotted in Figures A1–A2 in the Online Appendix. With different measurements of temperature, our main conclusion still holds, although the magnitude of the effect varies.

Lastly, we test for different functional forms of the dependent variable. The baseline model uses the logarithm of cropland area as the dependent variable, and thus the estimated coefficient is interpreted as a change of cropland area in percentage points. Alternatively, the original cropland area is included, so the estimates are measured in km^2. The results are still robust, as shown in Figure A3 in the Online Appendix. Taken together, we find a robust non-linear and long-lasting temperature effects on cropland area in China.

4.2 Heterogeneity by irrigation

Temperature may have heterogeneous effects on irrigated and non-irrigated cropland. Figure 6 plots the estimated coefficients and the 95% confidence intervals for irrigated land using the distributed-lag model. The effect of temperature bins above 30 ℃ on irrigated cropland is statistically insignificant in the first 5 years but becomes significantly negative from then on. This indicates that irrigation can mitigate the

negative effect of temperature rises in the short term (less than five years) but not in the long term (more than five years).

Figure 7 plots the estimated coefficients and the 95% confidence intervals for non-irrigated land using the distributed-lag model. Different from irrigated land, high temperatures have contemporaneous negative impact on non-irrigated land. The effects accumulate when more lags are included. The estimates using 10-year lags are similar between irrigated and non-irrigated lands, suggesting the role of irrigation in the adaption to hot weather in the long term is limited.

4.3 The impacts on other land types

Figure 8 plots the estimated coefficients and the 95% confidence intervals for developed land, which is the land used for urban and rural residence, infrastructure, and industry, using the distributed-lag model. The impact of temperature bins above 30 ℃ is small and insignificant for lags 0–2, but becomes statistically significant when more lags are included. The estimate in the 10-lag model suggests that a permanent change of one day from 15–20 ℃ to above 30 ℃ increases developed land area by 1% in 10 years. Given the negative impact of hot weather on cropland area, we can conclude that some lost cropland has been converted to developed land.

Figure 9 plots the estimated impacts on other land types, including forest land, grassland, waterbody, and barren land. To save space, we only report the estimates using 10-year lags. We also include cropland (irrigated and non-irrigated) and

developed land for comparison. Overall, we find insignificant impacts of hot weather on forest land, grassland, waterbody, and barren land.

4.4 Climate prediction

We predict the impacts of climate change by the end of this century (2070-2099) on cropland (irrigated and non-irrigated) using the historical response function between land area and temperature, as well as a set of downscaled climate models. To account for uncertainties in climate models (Burke et al., 2015), we use the average projection from 39 downscaled climate models from the Coupled Model Intercomparison Project 5 (Taylor et al., 2012). We focus on RCPs 2.6, 4.5, 6.0 and 8.5 in the Fifth Assessment Report (AR5) by the Intergovernmental Panel on Climate Change. RCP 2.6 is the slowest warming scenario while RCP 8.5 is the fastest one, with RCPs 4.5 and 6.0 in the middle.

We use the following method to do the climate prediction. First, we obtain the mean prediction on daily average temperature from 39 climate models for each month-grid over the periods 1970–2010 and 2070–2099. Second, we calculate the temperature difference in each month-grid between the two periods. Third, we add the difference to the observed daily time series from 1970–2010. This shifts the mean of daily temperature but also keeps its variance. Fourth, we calculate the predicted change in each 5 ℃ temperature bin. Finally, we multiply estimated coefficients from Equation (3) by the predicted change in each bin, and ultimately aggregate prediction on each bin to project the impacts of climate change on cropland.

Figure 10 depicts the estimated impacts in percentage points as well as 95% confidence intervals under the four RCPs. We find that climate change is likely to reduce China's cropland by 2.09 to 25.51%, depending on the RCPs. The estimates are statistically significant at 5% significance level under RCPs 4.5, 6.0, and 8.5. The predicted negative climate effects are similar for irrigated (2.06–19.44%) and non-irrigated (2.95–19.49%) cropland.

Using the relationship between climate and cropland, we can conduct a back-of-the-envelope calculation of the impact on food production. China produced 497 million tons of cereals in 2010 (FAO, 2010). If we assume agricultural productivity remains constant, a 25.51% loss in cropland area reduces cereals production by 126.78 million tons, or about 5% of global cereals production in 2010. China imported 5.69 million tons of cereals in 2010. To compensate for the loss of cereals production, China needs to increase cereals imports by 22 times, which is 37% of global exports of cereals.

Considering that climate change also has an adverse effect on agricultural productivity, the loss of food production will be even larger. Zhang et al. (2017) estimate that climate change is likely to decrease the yields of three major crops in China—rice, wheat, and corn—by 36.25%, 18.26%, and 45.10% respectively. Using the average crop yield loss (33.20%) and assuming the worst-case scenario of cropland loss (25.51%), climate change is likely to reduce China's total crop production by up to 50.24% by the end of this century. To compensate for this loss, China needs to import 250 million tons of cereals, which is nearly 10% of global cereals production and 74%

of global cereals exports in 2010. This will have a profound impact on the global food market.

Although this business-as-usual projection method is widely used in the climate-economy literature (e.g., Deschenes and Greenstone, 2007, 2011; Schlenker and Roberts, 2009), it bears several caveats. First, most climate-economy estimates based on historical data used short-term weather fluctuations, while climate change is permanent and gradual. We believe our estimates from Equations (1)–(3) partly alleviate this concern as we use three dynamic models to incorporate long-term temperature impacts.

Second, this projection assumes no price effect, constant population, economic growth, urbanization, and technology development. Here we discuss the possible effects if we change assumptions. If hot weather continues to negatively impact cropland, crop prices may be higher and thus more investment may be made and we may overestimate the cropland impacts. In terms of population, China's population is predicted to decrease from 1.38 billion in 2016 to 1 billion in 2100 (United Nations, 2017), which will relieve the pressure on crop demand in China. However, the global population is projected to increase from 7.44 billion in 2016 to 11.2 billion in 2100 (United Nations, 2015), implying keener competition with China for crop imports on the global market.

In terms of economic growth and urbanization, our projection may underestimate the true impact of climate change on cropland if the rate of economic

growth and urbanization keeps increasing since it will speed up the conversion of cropland to developed land, although the "red line" policy may mitigate the effect. As for technology development, our projection may overestimate the impact if heat-tolerant crops can be bred and promoted in the future.

5 Discussion

We find that extremely hot weather significantly reduces China's cropland. Climate change shifts the distribution of temperature to the right tail and leads to more extremely hot temperatures. Under the fastest warming scenario, climate change is likely to reduce China's cropland by 25.51% by the end of this century. Since China had 1.78 million km^2 of cropland in 2017, the loss is equivalent to 0.45 million km^2 cropland, which is almost as large as the total land area of Spain or Thailand, and larger than California.

We also find that adaptation through irrigation is unlikely to offset the negative effect: these croplands are either converted into developed land or become unsuitable for cropping in the long term. This conclusion is consistent with the previous findings in the U.S. that farmers are generally not able to adapt to climate change by maintaining the same crop yields in the long term (Schlenker and Roberts, 2009; Burke and Emerick, 2016).

High temperatures could affect cropland through two channels. The first channel is the active adjustment to high temperatures. If high temperatures lower

agricultural productivity, cropland may be converted to developed land for better value. The second channel is the passive adjustment to high temperatures. Extreme weather events such as heat waves or droughts may degrade cropland and make it unsuitable for cropping. China's "red line" policy, which has aimed to protect 1.2 million km^2 of cropland since 2006, can limit the active conversion of cropland to developed land through heavy regulations on land use. However, this policy cannot prevent high temperatures from making the cropland completely unsuitable for cropping. This may mean the Chinese government will need to augment the "red line" policy, either by introducing measures to guarantee a return on cropping such as providing subsidies to farming or increasing investment in infrastructure such as dams to deal with extreme weather events.

Most importantly, our results suggest that China should be more incentivized to reduce greenhouse gas (GHG) emissions in its own interest. China is the world's largest GHG emitter; China is also one of the most vulnerable countries in a warming world. Reducing GHG emissions is the ultimate approach to prevent further cropland loss to climate change.

Our method could be generalized to other settings. An international analysis could be implemented if fine spatiotemporal land data are available. However, two caveats exist in this study. First, we did not account for the CO_2 fertilization effect, since increasing CO_2 levels might spur crop growth and increase crop yields. We may overestimate the impact if the fertilization effect is significant. Second, we mainly

estimate the climatic impacts on cropland through increased temperatures. It is also possible that the rise in sea level will reduce cropland in coastal areas. In this case, our results may underestimate the climatic impacts on cropland. We will leave these questions for future research.

References

Auffhammer, Maximilian, Patrick Baylis, and Catherine H. Hausman. "Climate change is projected to have severe impacts on the frequency and intensity of peak electricity demand across the United States." *Proceedings of the National Academy of Sciences* 114, no. 8 (2017): 1886-1891.

Cressie, Noel, and Christopher K. Wikle. *Statistics for spatio-temporal data*. John Wiley & Sons, 2015.

Burke, Marshall, and Kyle Emerick. "Adaptation to climate change: Evidence from US agriculture." *American Economic Journal: Economic Policy* 8, no. 3 (2016): 106-40.

Burke, Marshall, John Dykema, David B. Lobell, Edward Miguel, and Shanker Satyanath. "Incorporating climate uncertainty into estimates of climate change impacts." *Review of Economics and Statistics* 97, no. 2 (2015): 461-471.

Dell, Melissa, Benjamin F. Jones, and Benjamin A. Olken. "Temperature shocks and economic growth: Evidence from the last half century." *American Economic Journal: Macroeconomics* 4, no. 3 (2012): 66-95.

Deschênes, Olivier, and Michael Greenstone. "The economic impacts of climate change: evidence from agricultural output and random fluctuations in weather." *American Economic Review* 97, no. 1 (2007): 354-385.

Deschênes, Olivier, and Michael Greenstone. "Climate change, mortality, and adaptation: Evidence from annual fluctuations in weather in the US." *American Economic Journal: Applied Economics* 3, no. 4 (2011): 152-85.

FAOSTAT, Food and Agriculture Organization of the United Nations. http://www.fao.org/faostat/en/data (2010).

Fezzi, Carlo, Amii R. Harwood, Andrew A. Lovett, and Ian J. Bateman. "The environmental impact of climate change adaptation on land use and water quality." *Nature Climate Change* 5, 255 (2015).

Larson, Christina. "Losing arable land, China faces stark choice: adapt or go hungry." *Science* (2013): 644-645.

Godfray, H. Charles J., John R. Beddington, Ian R. Crute, Lawrence Haddad, David Lawrence, James F. Muir, Jules Pretty, Sherman Robinson, Sandy M. Thomas, and

Camilla Toulmin. "Food security: the challenge of feeding 9 billion people." *Science* 327, no. 5967 (2010): 812-818.
Haim, David, Ralph J. Alig, Andrew J. Plantinga, and Brent Sohngen. "Climate change and future land use in the United States: an economic approach." *Climate Change Economics* 2, no. 01 (2011): 27-51.

Kyriakidis, Phaedon C. "A geostatistical framework for area-to-point spatial interpolation." *Geographical Analysis* 36, no. 3 (2004): 259-289.

Kong, Xiangbin. "China must protect high-quality arable land." *Nature* 506, no. 7486 (2014): 7.

Schlenker, Wolfram, and Michael J. Roberts. "Nonlinear temperature effects indicate severe damages to US crop yields under climate change." *Proceedings of the National Academy of sciences* 106, no. 37 (2009): 15594-15598.

Schmidhuber, Josef, and Francesco N. Tubiello. "Global food security under climate change." *Proceedings of the National Academy of Sciences* 104, no. 50 (2007): 19703-19708.

Taylor, Karl E., Ronald J. Stouffer, and Gerald A. Meehl. "An overview of CMIP5 and the experiment design." *Bulletin of the American Meteorological Society* 93, no. 4 (2012): 485-498.

Tol, Richard SJ. "The economic impacts of climate change." *Review of Environmental Economics and Policy* 12, no. 1 (2018): 4-25.

United Nations, Department of economic and social affairs, population division. world population prospects: The 2017 revision, methodology of the united nations population estimates and projections. esa/p/wp.242. (2017).

World Bank, 2019. https://data.worldbank.org/indicator/SP.POP.TOTL?locations=CN.

Zhang, Peng, Junjie Zhang, and Minpeng Chen. "Economic impacts of climate change on agriculture: The importance of additional climatic variables other than temperature and precipitation." *Journal of Environmental Economics and Management* 83 (2017): 8-31.

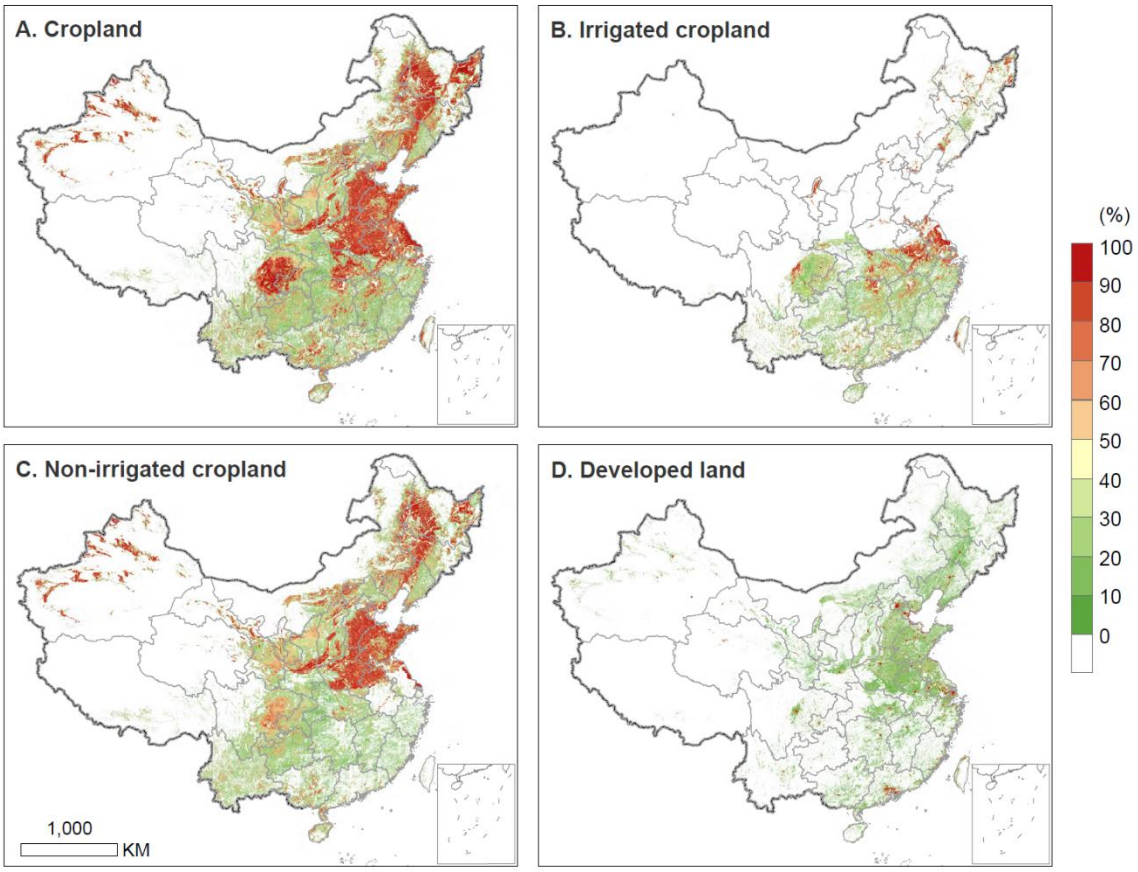

Figure 1: Geographic distribution of China's cropland and developed land in 2010.

Notes: The color shows the percentage of cropland (Panel A), irrigated cropland (Panel B), non-irrigated cropland (Panel C), and developed land (Panel D) in a 10×10-km grid.

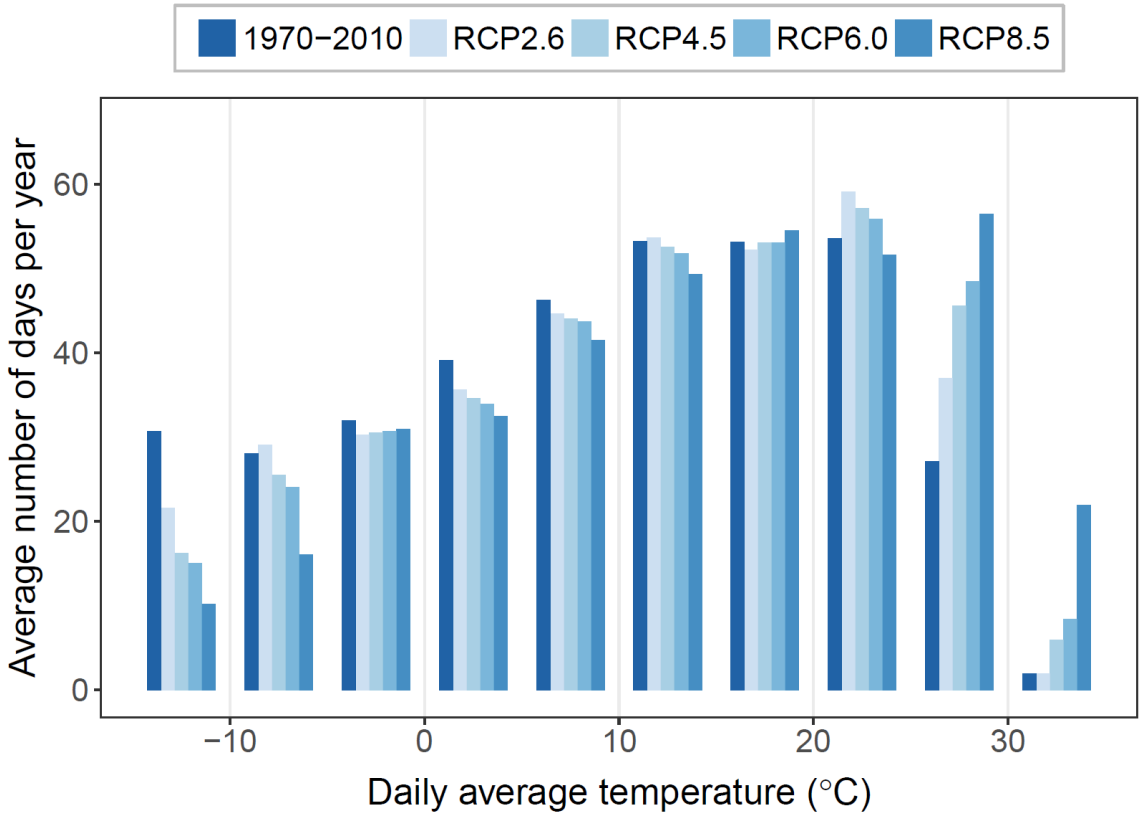

Figure 2: Temperature distribution under past (1970–2010) and future climate (2070–2099) under four RCPs.

Notes: The height of each bar denotes the average number of days with daily average temperature within each 5 ℃ interval in a year in China.

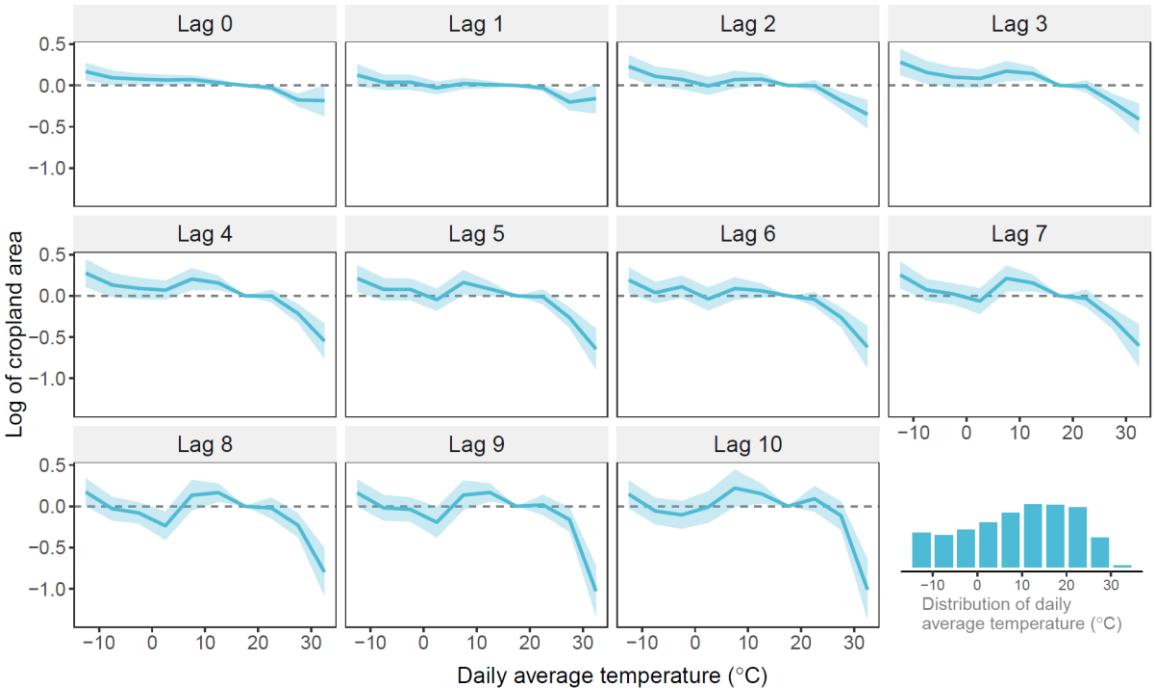

Figure 3: Estimated response function between cropland area (natural log) and daily average temperature using the distributed-lag model.

Notes: Each point estimate represents the cumulative effect of each temperature bin on cropland area up to 10 years. Temperature bin 15–20 ℃ is the reference group. The unit is percentage point. The control variables include second-order polynomials in annual cumulative precipitation, annual mean relative humidity, wind speed, and sunshine duration, grid fixed effect, and year-by-province fixed effect. The shaded area in light blue denotes the 95% confidence intervals, after adjusting for serial and spatial correlation within each grid.

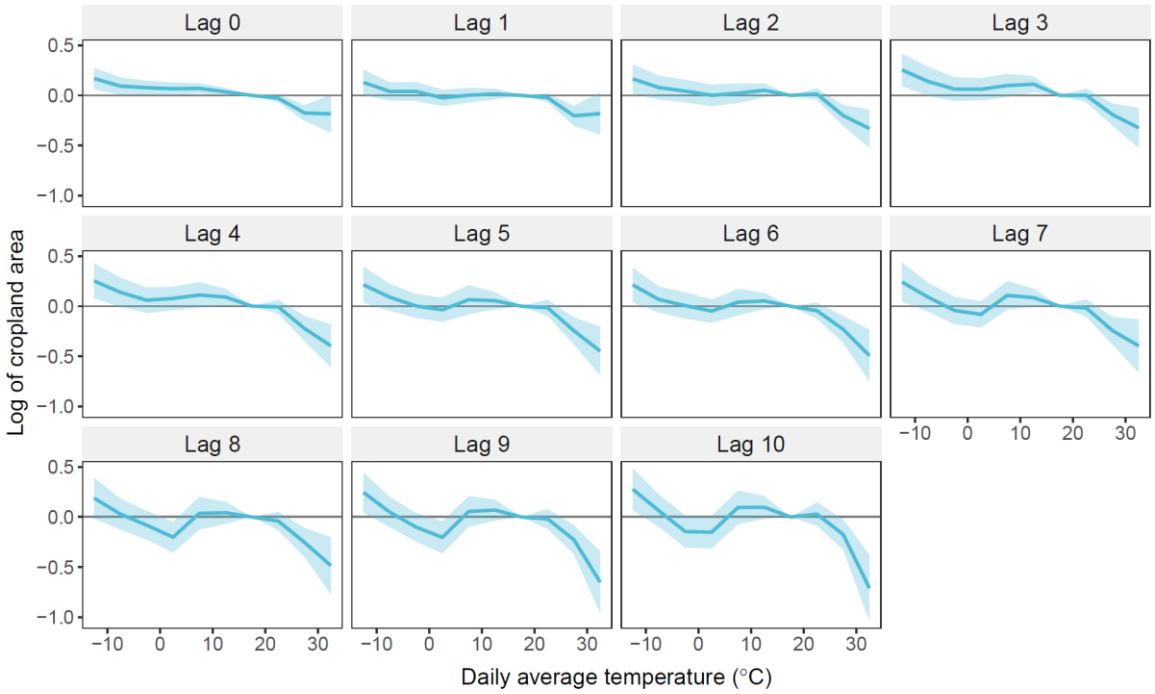

Figure 4: Estimated response function between cropland area (natural log) and daily average temperature using the period-averaged model.

Notes: Each point estimate represents the cumulative effect of each temperature bin on cropland area up to 10 years. Temperature bin 15–20 ℃ is the reference group. The unit is percentage point. The control variables include second-order polynomials in annual cumulative precipitation, annual mean relative humidity, wind speed, and sunshine duration, grid fixed effect, and year-by-province fixed effect. The shaded area in light blue denotes the 95% confidence intervals, after adjusting for serial and spatial correlation within each grid.

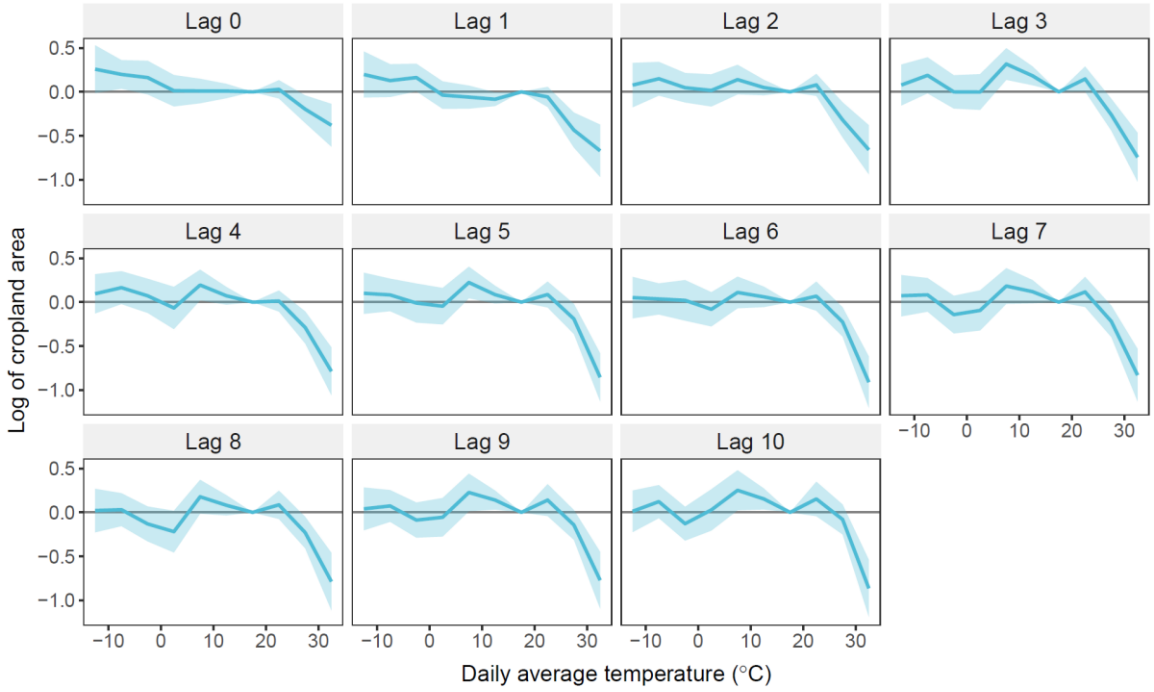

Figure 5: Estimated response function between cropland area (natural log) and daily average temperature using the long differences model.

Notes: Each point estimate represents the cumulative effect of each temperature bin on cropland area up to 10 years. Temperature bin 15–20 ℃ is the reference group. The unit is percentage point. The control variables include second-order polynomials in annual cumulative precipitation, annual mean relative humidity, wind speed, and sunshine duration, grid fixed effect, and year-by-province fixed effect. The shaded area in light blue denotes the 95% confidence intervals, after adjusting for serial and spatial correlation within each grid.

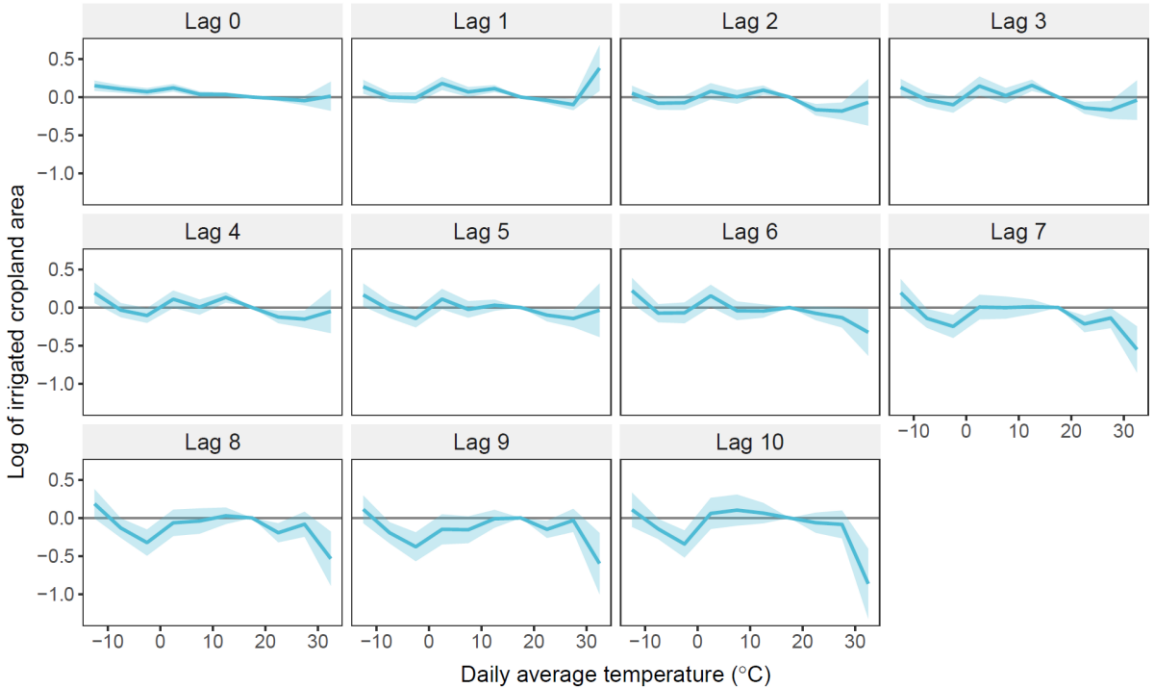

Figure 6: Estimated response function between irrigated cropland area (natural log) and daily average temperature using the distributed-lag model.

Notes: Each point estimate represents the cumulative effect of each temperature bin on irrigated cropland area up to 10 years. Temperature bin 15–20 ℃ is the reference group. The unit is percentage point. The control variables include second-order polynomials in annual cumulative precipitation, annual mean relative humidity, wind speed, and sunshine duration, grid fixed effect, and year-by-province fixed effect. The shaded area in light blue denotes the 95% confidence intervals, after adjusting for serial and spatial correlation within each grid.

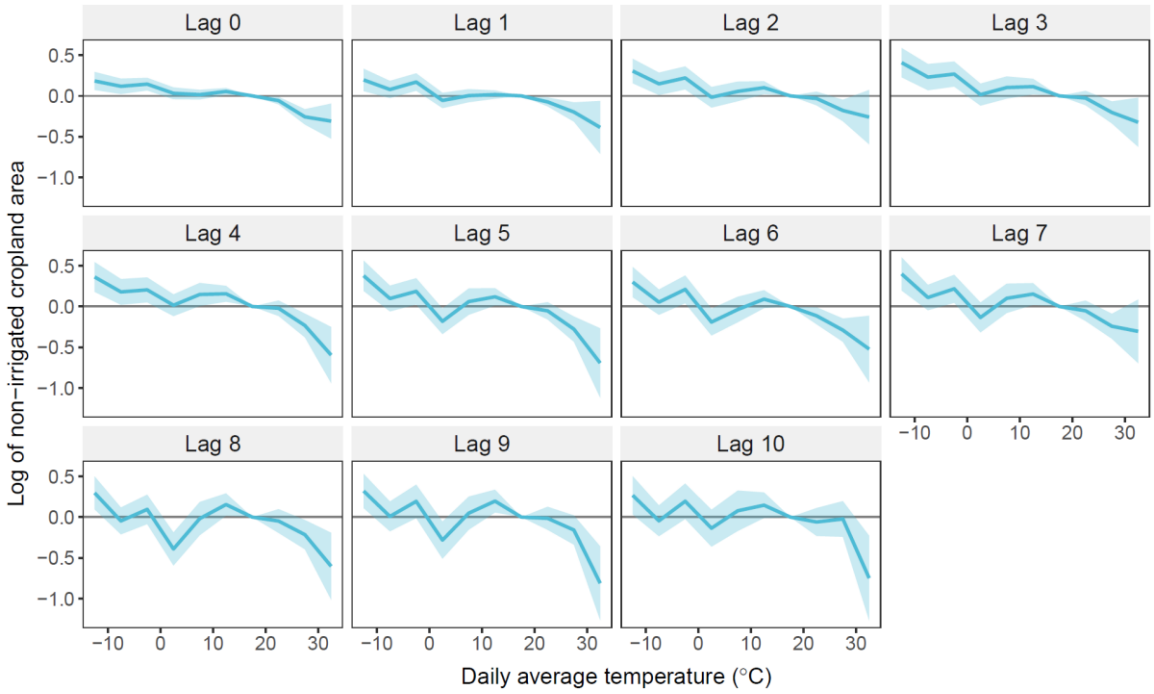

Figure 7: Estimated response function between non-irrigated cropland area (natural log) and daily average temperature using the distributed-lag model.

Notes: Each point estimate represents the cumulative effect of each temperature bin on non-irrigated cropland area up to 10 years. Temperature bin 15–20 ℃ is the reference group. The unit is percentage point. The control variables include second-order polynomials in annual cumulative precipitation, annual mean relative humidity, wind speed, and sunshine duration, grid fixed effect, and year-by-province fixed effect. The shaded area in light blue denotes the 95% confidence intervals, after adjusting for serial and spatial correlation within each grid.

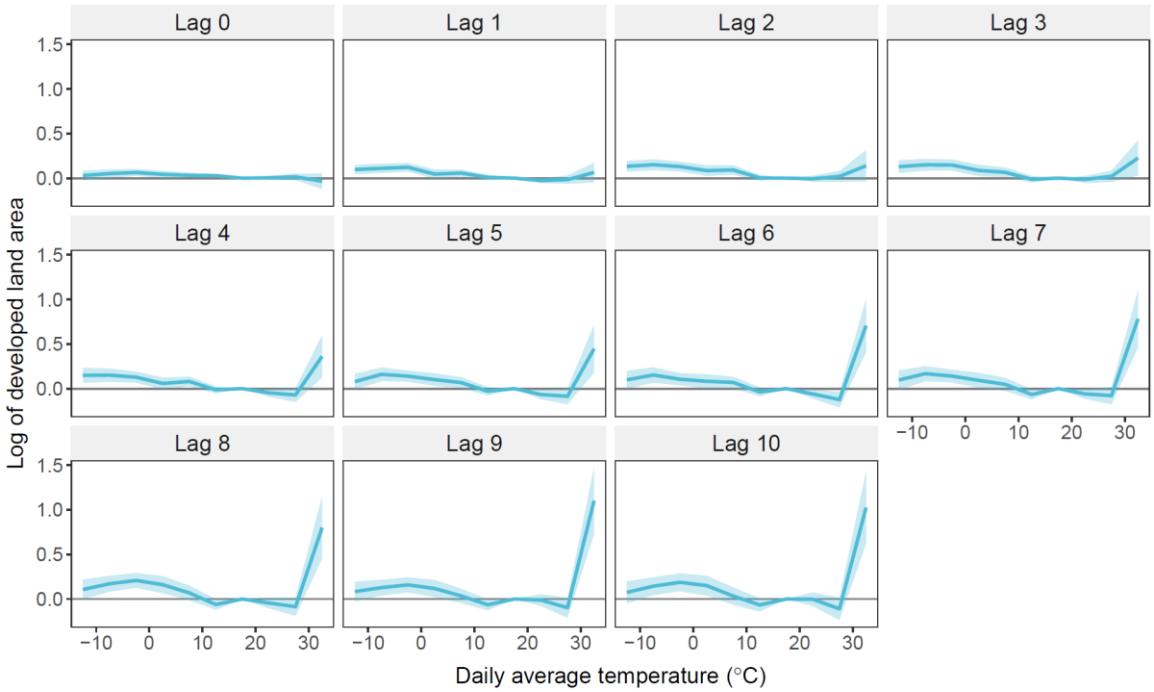

Figure 8: Estimated response function between developed land area (natural log) and daily average temperature using the distributed-lag model.

Notes: Each point estimate represents the cumulative effect of each temperature bin on developed land area up to 10 years. Temperature bin 15–20 ℃ is the reference group. The unit is percentage point. The control variables include second-order polynomials in annual cumulative precipitation, annual mean relative humidity, wind speed, and sunshine duration, grid fixed effect, and year-by-province fixed effect. The shaded area in light blue denotes the 95% confidence intervals, after adjusting for serial and spatial correlation within each grid.

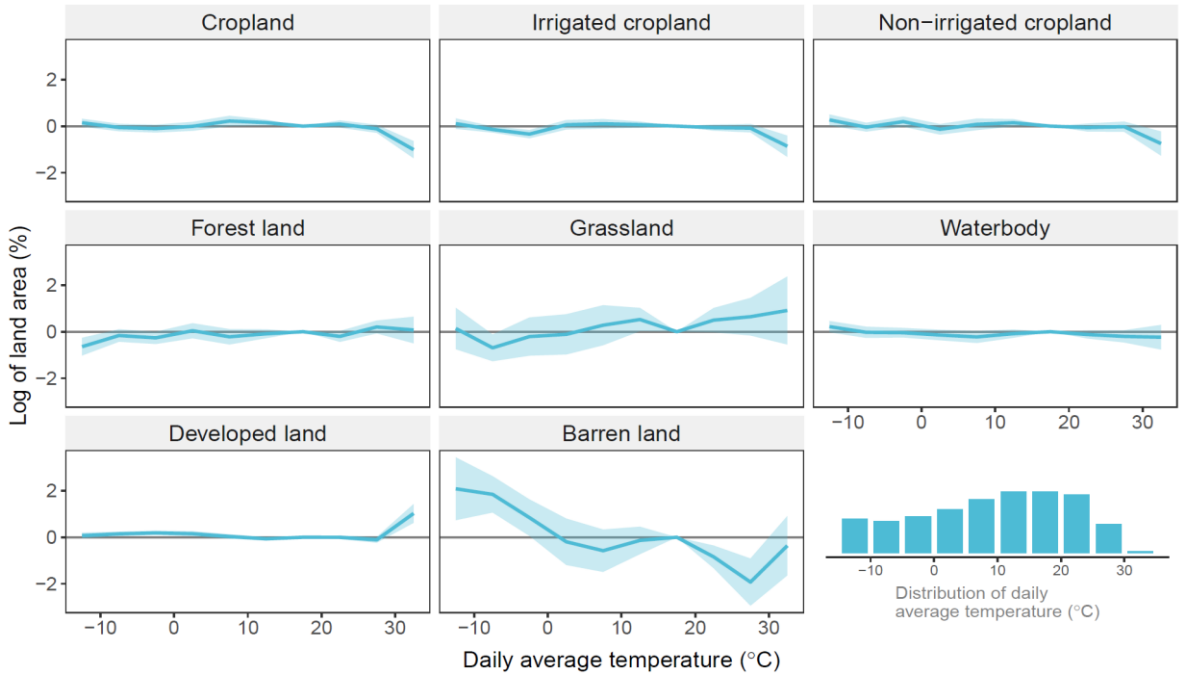

Figure 9: Estimated response function between different land area (natural log) and daily average temperature using the distributed-lag model with 10-year lags.

Notes: Each point estimate represents the cumulative effect of each temperature bin on different land area with 10-year lags. Temperature bin 15–20 ℃ is the reference group. The unit is percentage point. The control variables include second-order polynomials in annual cumulative precipitation, annual mean relative humidity, wind speed, and sunshine duration, grid fixed effect, and year-by-province fixed effect. The shaded area in light blue denotes the 95% confidence intervals, after adjusting for serial and spatial correlation within each grid.

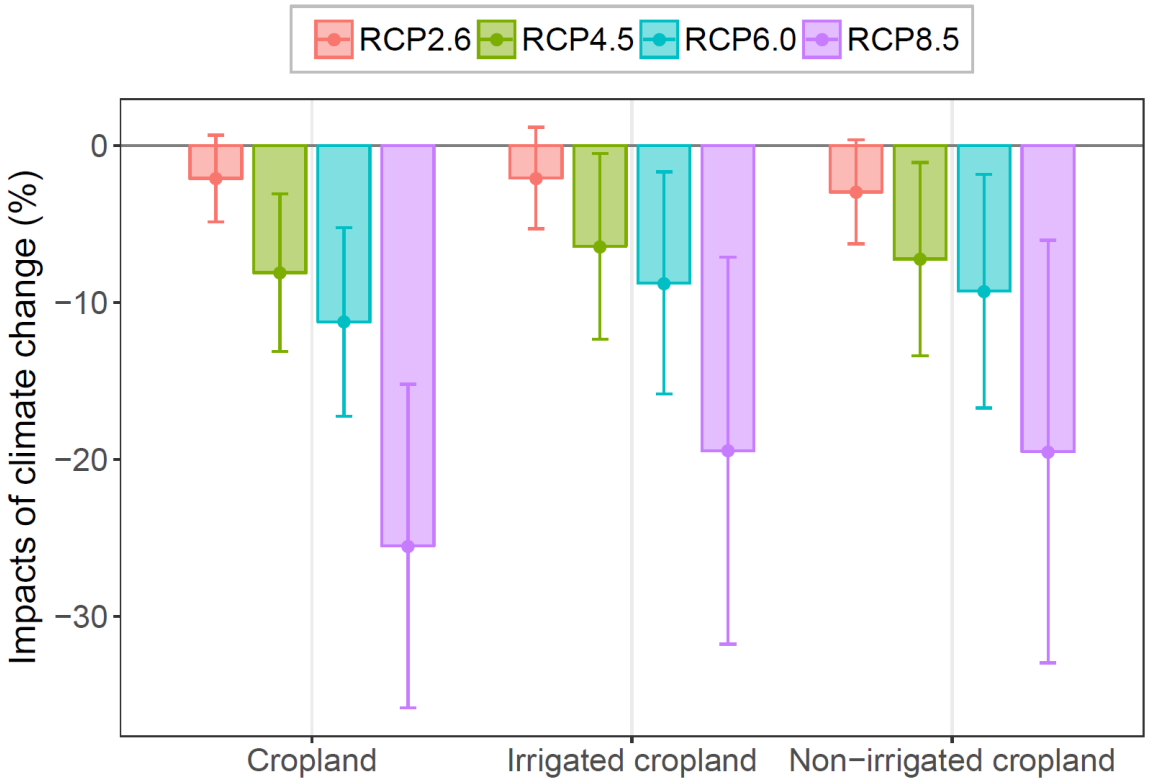

Figure 10: Predicted impacts of climate change (2070–2099) on cropland area under the mean projection from 39 climate models under four RCPs.

Notes: The climate impacts are calculated using the estimated regression coefficients of temperature on cropland area multiple by the predicted change in temperature. The unit is percentage point. The whiskers denote the 95% confidence intervals, after adjusting for spatial and serial correlation within each grid.

Table 1: Summary statistics

Variable	Unit	Mean	Std. Dev.	Min	Max
Panel A: Land	**km^2**				
Cropland		18.37	26.56	0.00	99.99
Irrigated land		4.61	12.40	0.00	99.22
Non-irrigated land		12.93	21.79	0.00	99.99
Developed land		1.88	5.29	0.00	100.00
Panel B: Temperature bins	**days**				
<–10 ℃		30.68	37.86	0.00	153.00
–10 – –5 ℃		28.06	23.67	0.00	94.00
–5–0 ℃		31.98	22.32	0.00	102.00
0–5 ℃		39.10	19.55	0.00	118.00
5–10 ℃		46.29	20.49	0.00	120.00
10–15 ℃		53.21	22.70	0.00	144.00
15–20 ℃		53.12	24.87	0.00	158.00
20–25 ℃		53.55	36.99	0.00	221.00
25–30 ℃		27.12	36.67	0.00	226.00
>30 ℃		1.89	4.64	0.00	35.00
Panel C: Other weather variables					
Precipitation	cm	59.82	51.49	1.00	262.71
Relative humidity	%	58.74	13.70	29.77	84.11
Sunshine duration	hour	6.81	1.68	2.40	9.69
Wind speed	m/s	2.33	0.57	0.93	4.42

Notes: N=482,105. Land data are reported within each 10×10-km grid. Temperature bins are number of days within each 5 ℃ using daily average temperature. Precipitation, relative humidity, sunshine duration, and wind speed are annual means.

Table 2: Regression results for weather variables other than temperature

	Lag 0	Lag 1	Lag 2	Lag 5	Lag 10
	(1)	(2)	(3)	(4)	(5)
Precipitation	-0.0593	-0.0107	0.0008	0.0142	0.0722
	(0.0511)	(0.0790)	(0.0798)	(0.1247)	(0.2121)
Precipitation^2	0.0002	-0.0000	-0.0002	-0.0003	-0.0005
	(0.0002)	(0.0003)	(0.0003)	(0.0004)	(0.0007)
Humidity	0.0863	0.3131	-0.4851	-0.4815	-2.0997
	(0.4389)	(0.4693)	(0.5511)	(0.6936)	(1.0255)
Humidity^2	-0.0002	-0.0034	0.0030	0.0054	0.0214**
	(0.0043)	(0.0047)	(0.0052)	(0.0062)	(0.0087)
Sunshine	-2.1685	0.0038	0.8066	0.9937	3.2596
	(2.9458)	(3.3594)	(3.4015)	(4.2496)	(5.2342)
Sunshine^2	0.3917**	0.2479	0.2219	0.2601	0.2426
	(0.1942)	(0.2260)	(0.2424)	(0.3261)	(0.3911)
Wind	-6.7501	-4.1009	-2.4772	-10.2576*	-27.7138***
	(4.3102)	(4.5860)	(4.6443)	(5.6086)	(8.0545)
Wind^2	0.9651	0.6767	0.1888	1.1312	3.8399***
	(0.7928)	(0.8478)	(0.8908)	(1.0440)	(1.4037)

Notes: N=482,105. The dependent variable is the log of cropland area. The model includes grid fixed effects and year-by-province fixed effects. This table supplements Figure 3 and reports regression results for weather variables other than temperature. Standard errors are clustered at the grid level and reported in parentheses. ***p<0.01, **p<0.05, *p<0.1.

Online Appendix

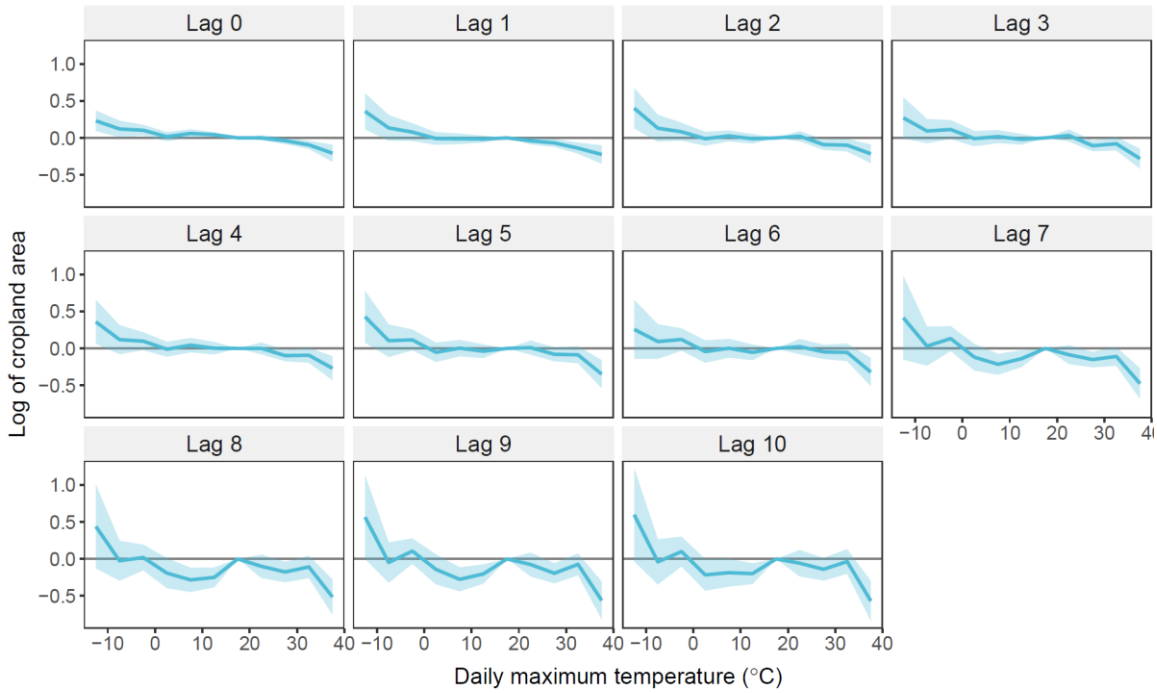

Figure A1: Estimated response function between cropland area (natural log) and daily maximum temperature using the distributed-lag model.

Notes: Each point estimate represents the cumulative effect of each temperature bin on cropland area up to 10 years. Temperature bin 15–20 ℃ is the reference group. The unit is percentage point. The control variables include second-order polynomials in annual cumulative precipitation, annual mean relative humidity, wind speed, and sunshine duration, grid fixed effect, and year-by-province fixed effect. The shaded area in light blue denotes the 95% confidence intervals, after adjusting for serial and spatial correlation within each grid.

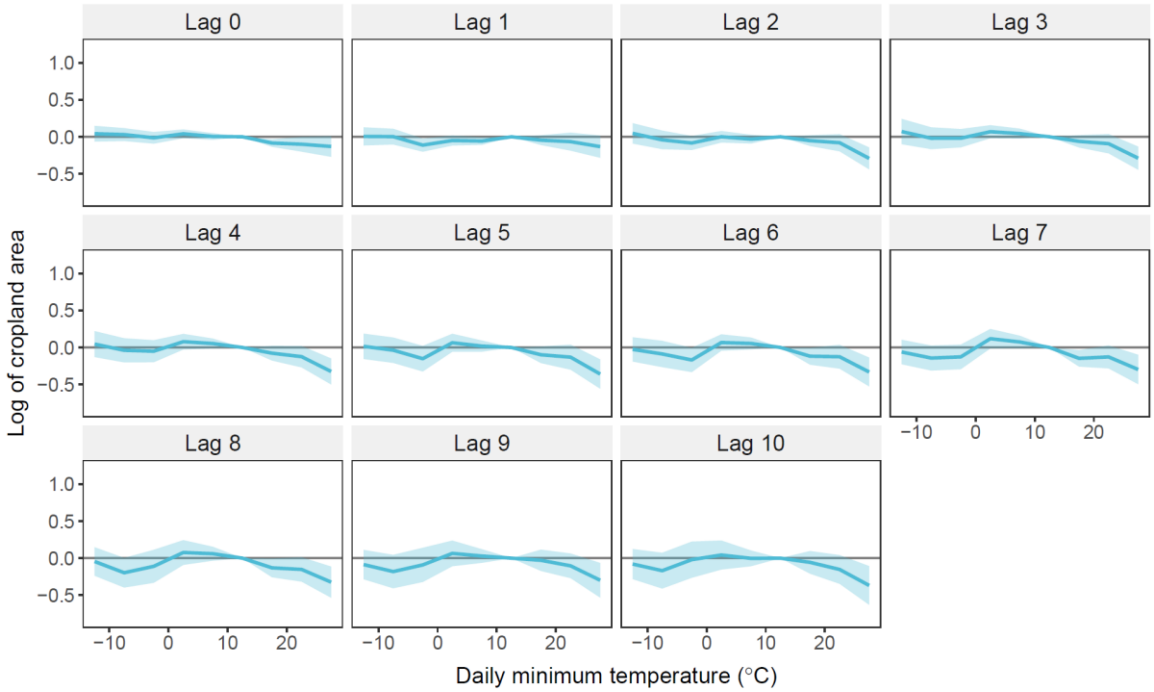

Figure A2: Estimated response function between cropland area (natural log) and daily minimum temperature using the distributed-lag model.

Notes: Each point estimate represents the cumulative effect of each temperature bin on cropland area up to 10 years. Temperature bin 10–15 ℃ is the reference group. The unit is percentage point. The control variables include second-order polynomials in annual cumulative precipitation, annual mean relative humidity, wind speed, and sunshine duration, grid fixed effect, and year-by-province fixed effect. The shaded area in light blue denotes the 95% confidence intervals, after adjusting for serial and spatial correlation within each grid.

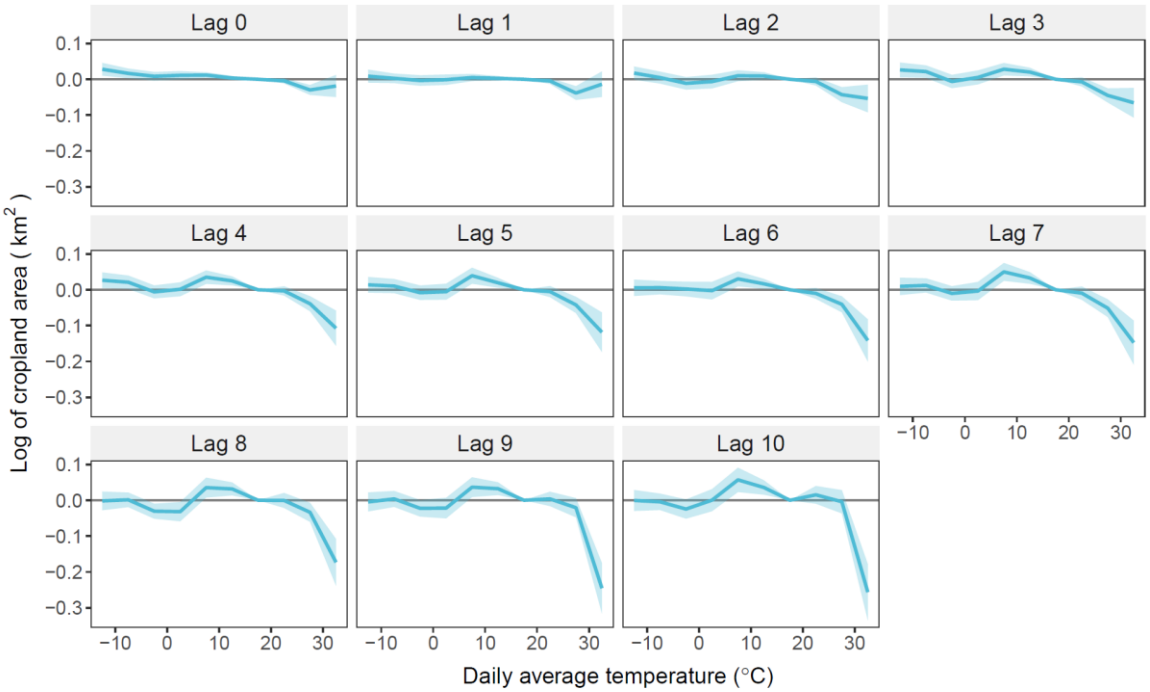

Figure A3: Estimated response function between cropland area (in level) and daily average temperature using the distributed-lag model.

Notes: Each point estimate represents the cumulative effect of each temperature bin on cropland area up to 10 years. Temperature bin 15–20 ℃ is the reference group. The unit is km^2. The control variables include second-order polynomials in annual cumulative precipitation, annual mean relative humidity, wind speed, and sunshine duration, grid fixed effect, and year-by-province fixed effect. The shaded area in light blue denotes the 95% confidence intervals, after adjusting for serial and spatial correlation within each grid.